Materials Research Proceedings 44 (2024) 90-99 https://doi.org/10.21741/9781644903254-10

Experimental formability evaluation for aluminium alloy sheets under hot stamping conditions

ZHANG Ruiqiang[1,a *], LI Jiaqi[1,b], SHI Zhusheng[1,c] and LIN Jianguo[1,d]

[1]Department of Mechanical Engineering, Imperial College London, London SW7 2AZ, UK

[a]r.zhang17@imperial.ac.uk, [b]jiaqi.li120@imperial.ac.uk, [c]zhusheng.shi@imperial.ac.uk, [d]jianguo.lin@imperial.ac.uk

Keywords: Aluminium Alloy, Hot Stamping, Formability, Necking, Fracture, Forming Limit Curves

Abstract. The process of Hot Form and Quench for aluminium alloys, known as HFQ®, has been developed and applied to manufacture lightweight, high-strength engineering panel components in the automotive industry. However, formability evaluation for the alloys under hot stamping conditions is challenging. In this study, a recently developed biaxial testing method has been applied to aluminium alloy AA6082 for formability evaluation at temperatures ranging from 440–510 °C and at a strain rate of 0.1 s^{-1}. This method involves heating cruciform specimens via the resistance heating system in the Gleeble, and deforming them until fracture via a customised biaxial tensile rig which transfers a uniaxial force into biaxial forces. The location for welding thermocouples on cruciform specimen surface for temperature feedback control in the Gleeble is investigated. Furthermore, temperature nonuniformity within the gauge area of cruciform specimens is quantified, and biaxial tensile tests on the specimens are carried out under different conditions. Both the limit strains at the onset of necking and at fracture are determined, and their dependency on the deformation conditions is analysed. It is found that the biaxial testing method is applicable to AA6082 for formability evaluation under hot stamping conditions. In addition, the limit major strains vary with the strain state, but exhibit a minor dependency on the temperature in the range investigated.

Introduction

Hot Form and Quench (HFQ®) for aluminium alloys is a hot stamping process for manufacturing lightweight, high-strength panel components for a wider range of industrial applications [1]. During the processes, the alloy is heated for solution heat treatment, and then quickly transferred into cold process dies for simultaneous forming and in-die quenching, followed by artificial aging to obtain the highest strength because of the precipitate hardening [2, 3]. Numerical simulations of hot stamping processes are essential to the design and optimisation of these processes [4, 5]. For accurate numerical simulations, it is essential to determine the thermo-mechanical properties of the alloy under hot stamping conditions for the development and calibration of materials constitutive models [6-8].

Formability refers to the capability of an alloy to undergo plastic deformation without experiencing failure [9]. Forming limit curves (FLCs) are the most widely used tools to quantitively evaluate the formability for sheet metals, which are constructed using the limit strains at the onset of necking in various strain states from uniaxial over plane-strain to equi-biaxial tensions [10-12]. Fracture forming limit curves (FFLCs) are more recently developed tools, which are constructed using the limit strains at fracture [13]. The Nakajima tests have been widely carried out to determine FLCs of sheet metals at room temperature [14-16], and even at high temperatures [17-19]. In the Nakajima tests, sheet metals are deformed by a hemispherical punch through thickness direction [20]. In order to reduce the friction between the punch and the blank, a suitable lubricant system should be applied, so that the fracture of the blank occurs within a certain region

[20]. For high temperature tests, the blank is heated in furnaces. However, due to the challenge to replicate the intricate thermal cycle in hot stamping, and the failure of lubricant system at high temperatures, it is extremely difficult to apply the Nakajima tests to determine FLCs and/or FFLCs for sheet metals under hot stamping conditions.

Recently, a biaxial testing method has been developed and successfully applied to boron steel for the determination of both FLCs and FFLCs under hot stamping conditions [21]. In this testing method, a type of cruciform specimen was designed, and heated using the resistance heating method. By leveraging the feedback control heating system in the Gleeble thermo-mechanical simulator, it has been found that the intricate thermal cycle for hot stamping can be replicated accurately. In addition, since the specimens are stretched in plane-stress state, lubricant systems are not required anymore as in the Nakajima tests. However, the applicability of the biaxial testing method to aluminium alloys, such as the cruciform specimen design and the heating method, is still unknown.

The present study aims to apply the newly developed biaxial testing method to aluminium alloy AA6082 for the determination of both FLCs and FFLCs under hot stamping conditions. Cruciform specimens of AA6082 are heated using the resistance heating method, and stretched under different loading, temperature and strain rate conditions. The digital image correlation (DIC) is applied to measure the full-field strain within the gauge area of the specimens. The strain data are consequently post-processed to determine the limit strains at necking and fracture for constructing both FLCs and FFLCs.

Methodology

Material and thermal cycle for hot stamping. Aluminium alloy AA6082 sheets with an initial thickness of 1.5 mm are used in the present study. The composition of the alloy is Al-0.87Si-0.33Fe-0.026Cu-0.51Mn-0.97Mg-0.044Cr0.025Zn-0.016Ti (wt. %). Fig. 1 shows the temperature cycle of AA6082 which mimics the conditions during industrial hot stamping processes. The alloy is heated to 535 °C and soaked at this temperature for 60 s to generate supersaturated solid solution. Subsequently, the alloy is quenched at 60°C/s to the target forming temperature for thermo-mechanical deformation.

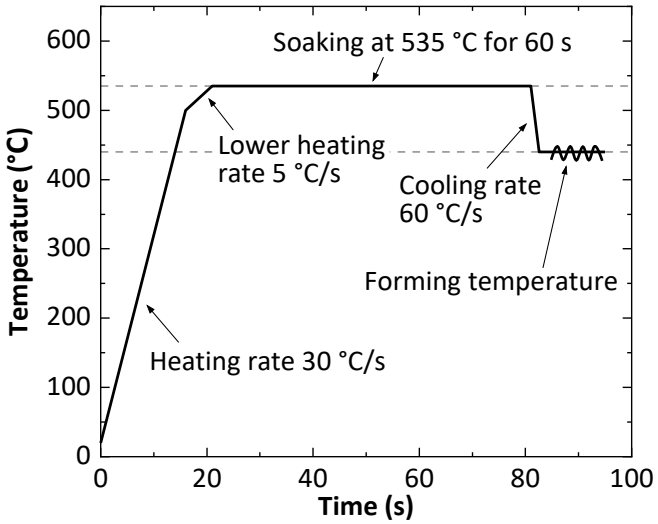

Fig. 1. Temperature cycle for AA6082 for hot stamping.

Biaxial testing method. The biaxial testing method, originally developed in Ref. [21], is applied to AA6082 for formability evaluation under hot stamping conditions in the present study. Fig. 2(a) shows the schematic diagram of utilising this biaxial testing method to determine forming limit curves (FLCs) and fracture forming limit curves (FFLCs) for the alloy. In this method, a biaxial

tensile system is used to heat and stretch cruciform specimens under various loading conditions. The biaxial tensile system consists of a Gleeble thermo-mechanical simulator and a customised biaxial tensile rig. During the testing, the biaxial tensile rig is installed inside the chamber of the Gleeble, as shown in Fig. 2(b), and transfers, through slider-crank mechanisms, uniaxial forces provided by the Gleeble into biaxial forces for stretching cruciform specimens. The Gleeble also provides electric currents to heat the specimens using the resistance heating method to precisely achieve the complex temperature cycle including rapid heating and quenching as shown in Fig. 1. During the deformation of the specimens, the strain fields within the gauge area are measured using the digital image correlation (DIC), and consequently post-processed using the spatio-temporal method, originally developed in Ref. [22], to determine the limit strains at the onset of necking and at fracture. Finally, those limit strains are used to construct both FLCs and FFLCs. Fig. 1(c) shows the experimental setup for formability evaluation, including the Gleeble, the high-speed camera (Photron FASTCAM Mini delivering 1,280 by 1,024 pixel resolution) for DIC, and the biaxial tensile rig together with the cruciform specimen, etc. Fig. 2(d) presents the geometry and dimensions of the cruciform specimen, originally developed in Ref. [21, 23], and its heating scheme. The gauge area of each specimen is located in the centre, and is intentionally thinned into a domed shape to concentrate and localise deformation within this region. Regarding the heating scheme, the upper arm of each specimen is connected to the positive electrode, and the lower arm is connected to the negative electrode. During the testing, electrical currents provided by the Gleeble, flow through the specimen and heat the specimen based on the phenomena of joule heating.

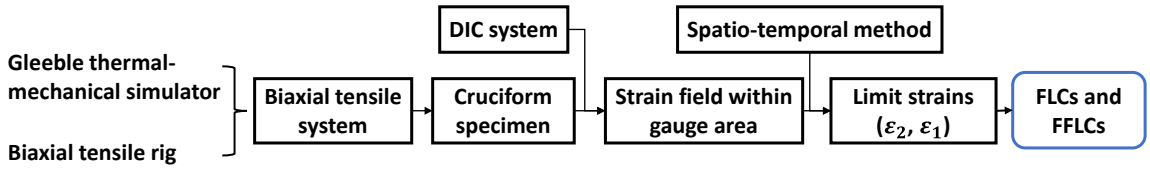

(a)

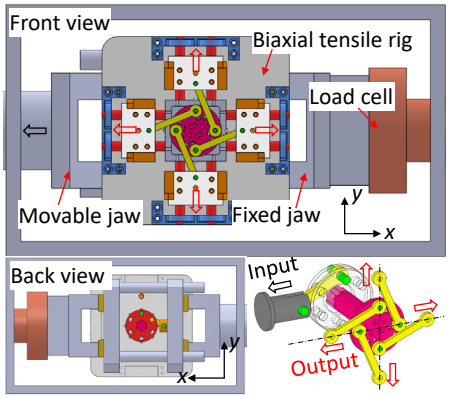

(b)

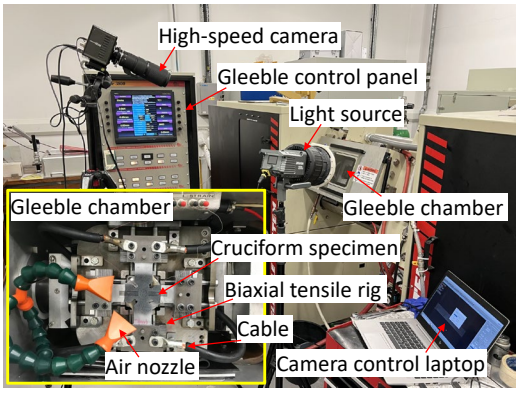

(c)

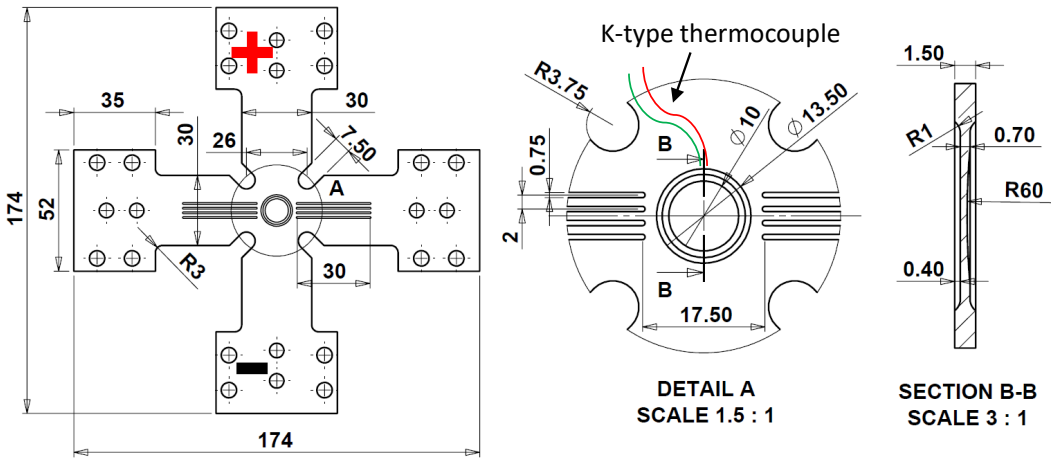

(d)

Fig. 2. Biaxial testing method for formability evaluation under hot stamping conditions, (a) Schematic diagram of utilising the biaxial testing method to determine forming limit curves (FLCs) and fracture forming limit curves (FFLCs), (b) Experimental setup, (c) Biaxial tensile rig and its setup in the Gleeble, and (d) Geometry and dimensions (unit: mm) of the cruciform specimen. Symbols '+' and '–' mean connecting positive and negative electrode, respectively.

Regarding the strain measurement using DIC, in the present study, a region of 35 mm by 28 mm on specimen surface which covers the gauge area throughout the deformation was recorded using the high-speed camera. The pictures were post-processed using the commercial software GOM Correlate 2018, with setting facet size to 19 pixels and point distance to 10 pixels.

Table 1 lists all testing conditions for formability evaluation in the present study, including loading state, temperature and strain rate. Each test was repeated twice to enhance the accuracy and reliability of the data obtained.

Table 1. Testing conditions for biaxial tensile tests for formability evaluation.

Test	Loading state	Temperature (°C)	Equivalent strain rate (s^{-1})
1	Equi-biaxial	440	0.1
2	Plane-strain	440	0.1
3	Uniaxial	440	0.1
4	Equi-biaxial	510	0.1
5	Plane-strain	510	0.1
6	Uniaxial	510	0.1

Results

Temperature distributions. It is well known that the heating system in the Gleeble results in a nonuniform temperature distribution within the gauge area of the specimen [24]. The temperatures at the locations A, B, and C, as indicated in Fig. 3, were therefore measured and quantified by using K-type thermocouples welded at these locations. Fig. 3 shows the results when controlling the temperature at A to reproduce the target temperature cycle specified in Fig. 1. As can be seen, the target temperature cycle at A was reproduced precisely. Furthermore, after the temperature stabilises, the location A has the highest temperature, followed by B and then C. As indicated in Fig. 2(d), in the present study, the measured temperature cycle at B was used to indirectly control the temperature at A. Additionally, the stabilised temperatures at B and C were quantified when the stabilised temperature at A reached different values. Table 2 lists the results. As can be seen, the difference between the temperatures at A and C, which represent the maximum temperature difference within the gauge area [21], is less than 20°C.

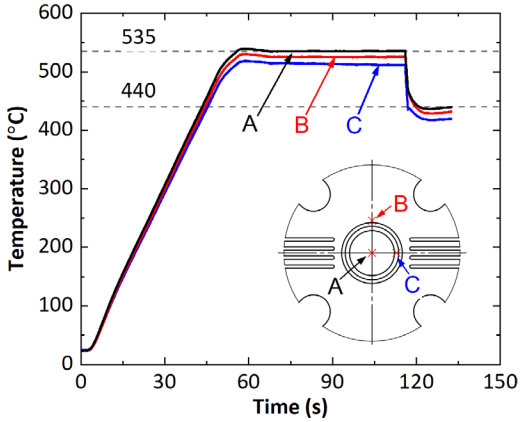

Fig. 3. Temperature distribution in the intersection region of the cruciform specimen, with an inset showing the locations of A, B and C.

Table 2. Stabilised temperature (°C) at the locations A, B and C of cruciform specimen during soaking and deformation. Different cases mean the stabilised temperature at A reaching different values.

Location	Case I	Case II	Case III	Case IV
A	535	510	440	370
B	525	498	432	361
C	513	490	420	357

Fracture cruciform specimens. Fig. 4 shows the fractured cruciform specimens of AA6082 under the different conditions listed in Table 1. As can be seen, the fracture occurred near the specimen centre in all the tests. This indicates the effectiveness of the specimen design for evaluating the formability for AA6082 [25], similarly to the applications to boron steel [21].

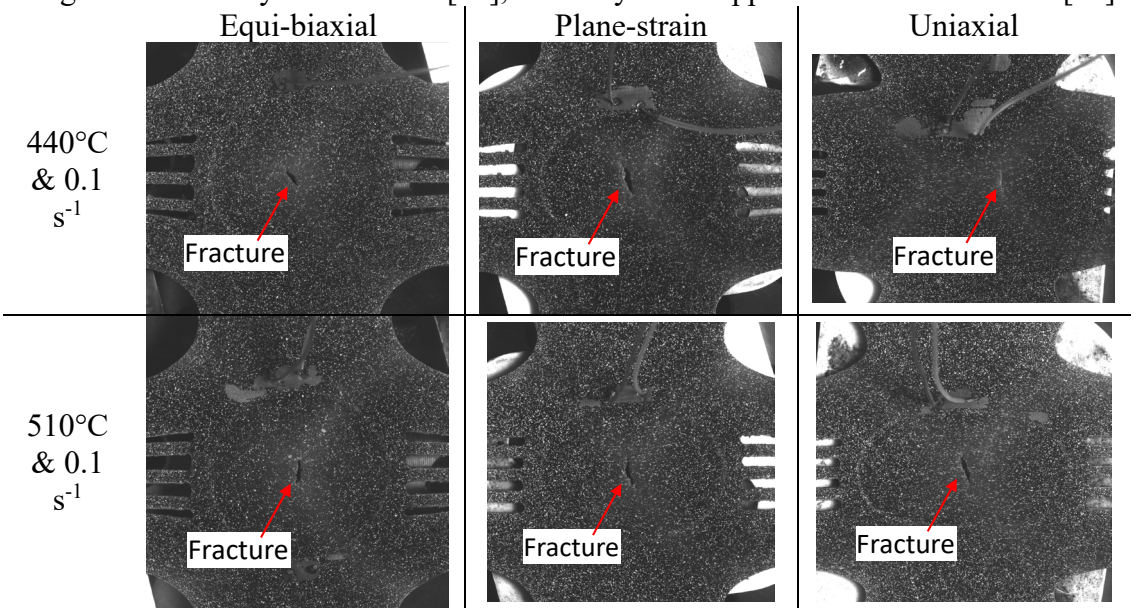

Fig. 4. Fractured cruciform specimens of AA6082 at different temperatures and strain rates.

Fig. 5 shows the total force applied to the biaxial tensile rig for stretching these cruciform specimens until the fracture; the force was measured by the load cell as indicated in Fig. 2(b). As can be seen, the force required to induce fracture in the specimens in plane-strain tension is smaller than that in plane-strain tension but higher than that in uniaxial tension. Additionally, a higher

temperature results in lower forces needed to fracture the specimens. Similar phenomenon was observed in the applications to boron steel [21]. However, the fracture force required for AA6082 is significantly less than that for boron steel.

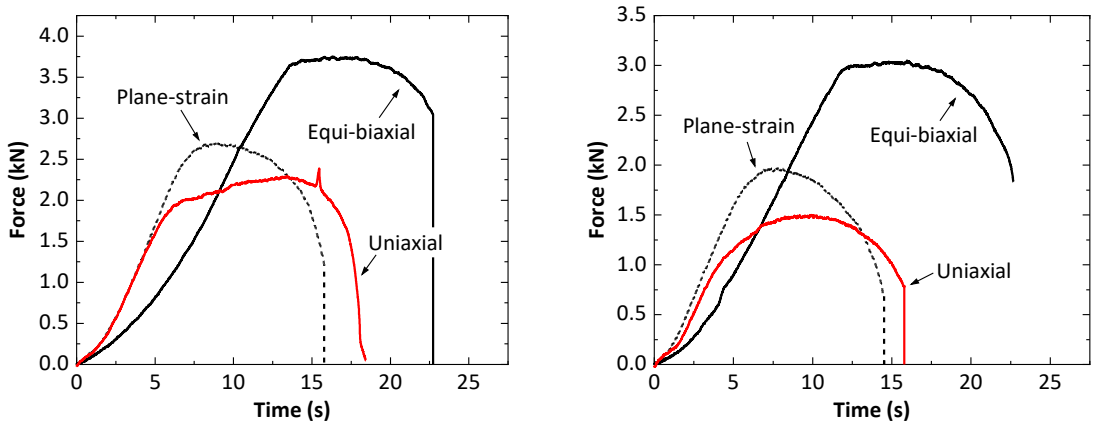

Fig. 5 Total force applied to the biaxial tensile rig for stretching the cruciform specimens at (a) 440°C and 0.1 s^{-1} and (b) 510°C and 0.1 s^{-1}.

Fig. 6 shows the strain fields within the gauge area of the specimens, measured using DIC, in different loading states at 510°C and 0.1 s^{-1}. The percent values 0%, 50%, 80% and 98% represent the time normalised by the time at fracture. As can be seen, the full field strains within the gauge area before 98% were successfully measured in all the cases. Furthermore, as the time increases, the deformation within the gauge area increases, especially in the vicinity of the specimen centre. This is attributed to the nonuniform thickness (Fig. 2(d)) and the temperature distribution (Fig. 3) within the gauge area.

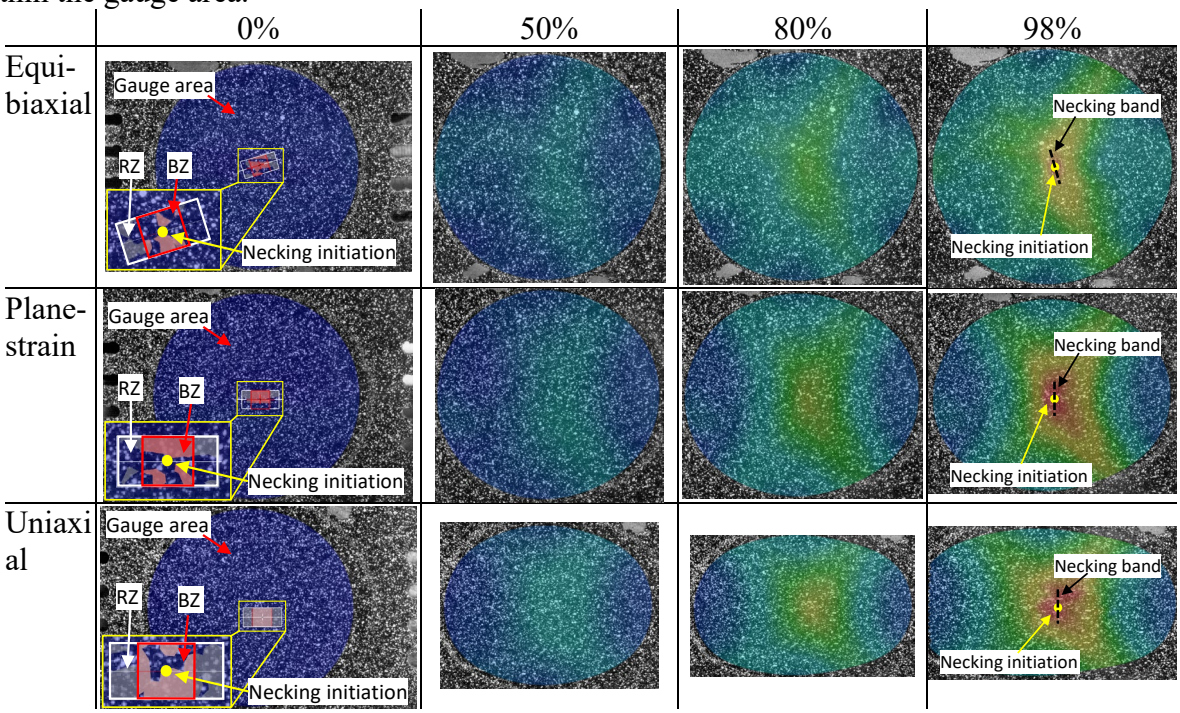

Fig. 6. Evolution of the strain fields in the gauge area of the cruciform specimens deformed in different loading states at 510°C and 0.1 s^{-1}. The percent values 0%, 50%, 80% and 98% represent the times normalised by the time at fracture.

FLCs and FFLCs for AA6082. Based on the strain fields measured using DIC, the limit strains at the onset of necking and at fracture were determined by using the spatio-temporal method. To apply this method, a base zone (BZ) and a reference zone (RZ) were selected around the location where necking occurred, as shown in Fig. 6. Both zones have the same size along the localised necking band, but differ in the dimension perpendicular to the band. Specifically, the initial size of BZ is 1.1 mm by 1.1 mm, while the size of RZ is 2.2 mm by 1.1 mm [21]. Fig. 7(a1), (b1) and (c1) shows the thinning within BZ against the thinning within RZ in different loading states at 510°C and 0.1 s^{-1}. Bilinear fitting was applied to the thinning data, both during the initial stages and the later stages of deformation. Subsequently, the onset of localised necking was identified at the intersection of the fitted lines. Fig. 7(a2), (b2) and (c2) shows the limit strains determined using the spatio-temporal method, together with the strain paths until fracture. Among the three strain states presented, the strain path obtained in equi-biaxial tension demonstrates the best linearity, with the associated strain ratio of approximately 0.6.

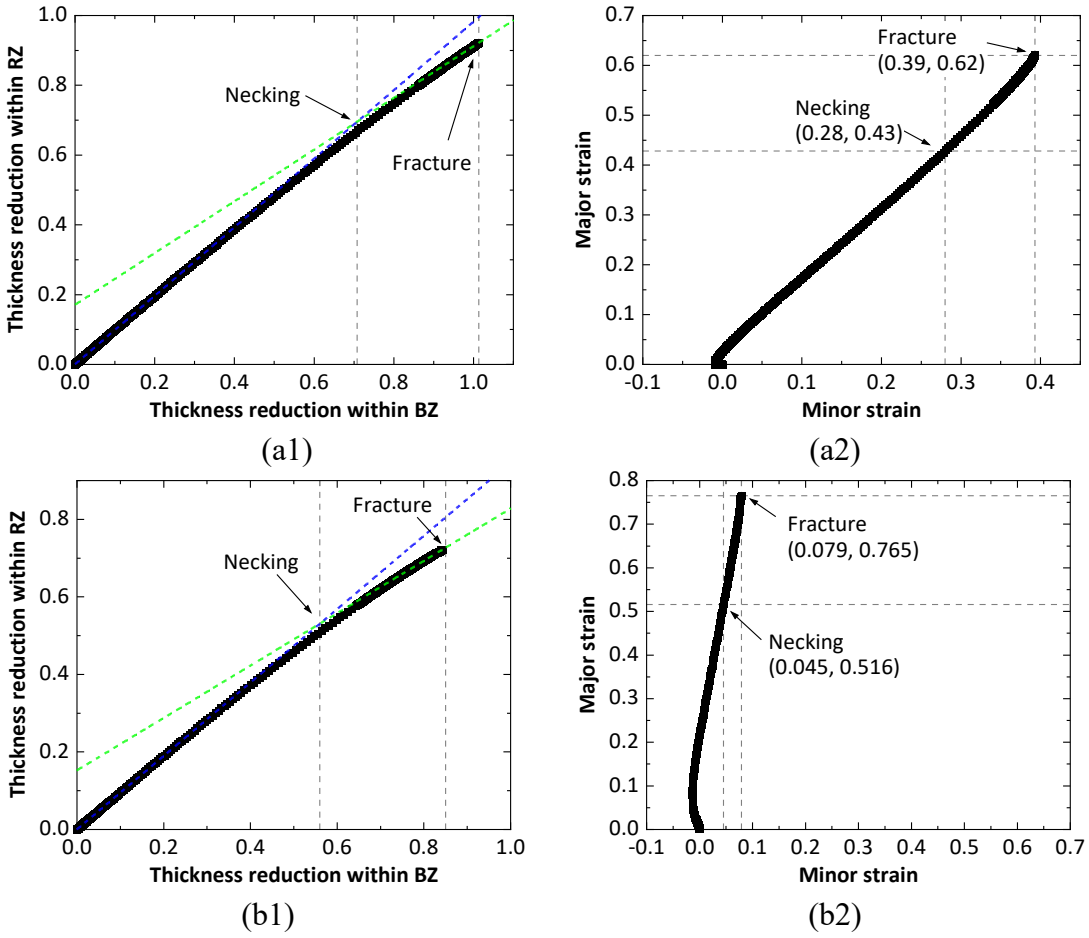

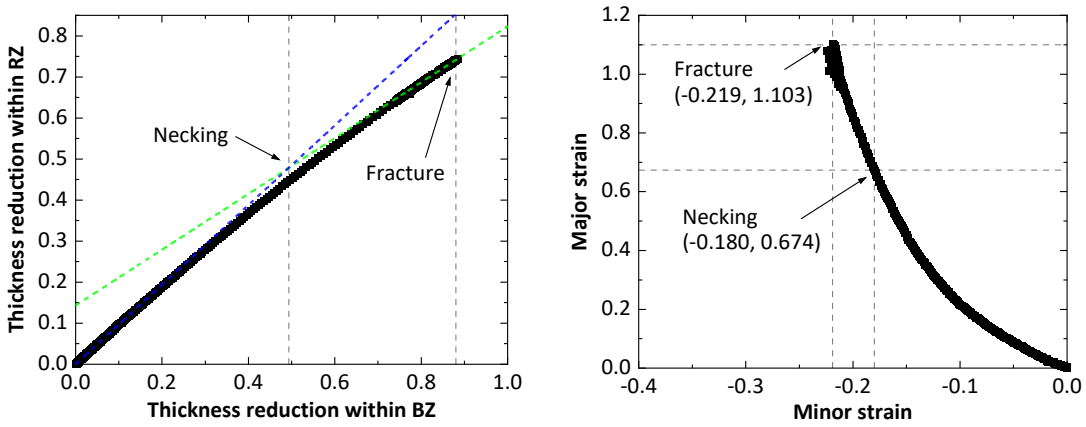

(c1) (c2)

Fig. 7. Determination of the limit strains at the onset of necking and at fracture using the spatio-temporal method for the specimens deformed at 510°C and 0.1 s^{-1}: the thinning within the base zone (BZ) against the reference zone (RZ) in (a1) equi-biaxial, (b1) plane-strain and (c1) uniaxial tensions, and the strain paths with the determined limit strains in (a2) equi-biaxial, (b2) plane-strain and (c2) uniaxial tensions.

Fig. 8 shows the collated limit strains at necking for FLCs and at fracture for FFLCs for AA6082 at 440°C and 0.1 s^{-1} and at 510°C and 0.1 s^{-1}, determined using the biaxial testing method in the present study. As can be seen, the limit major strain values at both necking and fracture are dependent on strain state; they are the highest in uniaxial tension, and decrease at a decreasing rate as the strain ratio increases. Additionally, the limit strain values are slightly dependent on the deformation temperature in the range investigated (i.e. 440–510°C) in the present study.

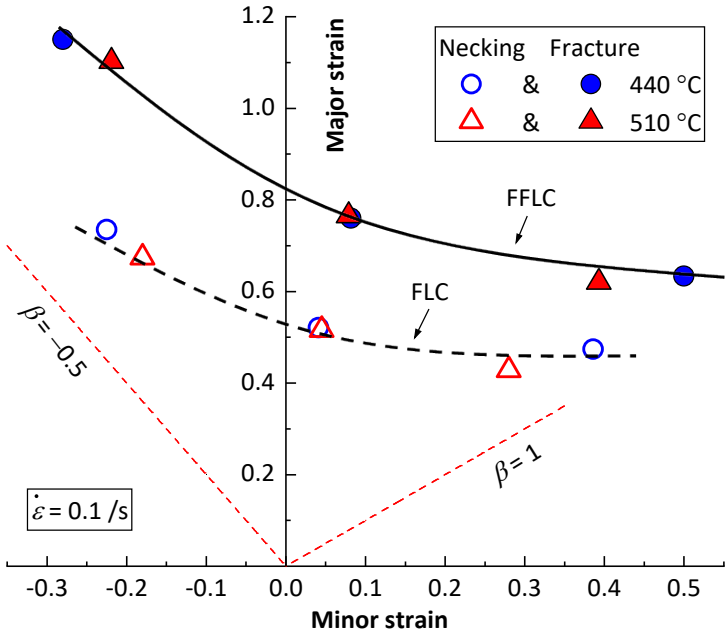

Fig. 8. Determined limit strains at necking for constructing forming limit curves (FLCs) and limit strains at fracture for constructing forming limit curves (FFLCs) for AA6082 under hot stamping conditions.

Conclusion

The formability of AA6082 sheets under hot stamping conditions at 440-510°C and 0.1 s^{-1} has been successfully evaluated using a recently developed biaxial testing method. The maximum

temperature difference within the gauge area of the cruciform specimen is approximately 20°C. Furthermore, this testing method ensures the fracture initiation near the specimen centre, contributing to achieving almost linear strain paths with target strain ratios. The determined limit strains at both necking and fracture depend on the strain states, with a minor dependency on the deformation temperature investigated in this study.

Acknowledgement
This work was supported by the Engineering and Physical Sciences Research Council (EPSRC) [Grant number EP/R001715/1] on "Lightform: Embedding Materials Engineering in Manufacturing with Light Alloys".

References

[1] J. Lin, T.A. Dean, R.P. Garrett, A.D. Foster, Process for forming metal alloy sheet components, International 'Patent' WO 2008059242 A2, (2008), May 22, 2008.

[2] K. Zheng, Y. Dong, J.-H. Zheng, A. Foster, J. Lin, H. Dong, T.A. Dean, The effect of hot form quench (HFQ®) conditions on precipitation and mechanical properties of aluminium alloys, Mater. Sci. Eng. A 761 (2019). https://doi.org/10.1016/j.msea.2019.06.027

[3] ASM Handbook, Heat Treating of Aluminum Alloys, 1991.

[4] Z.W. Xing, J. Bao, Y.Y. Yang, Numerical simulation of hot stamping of quenchable boron steel, Mater. Sci. Eng. A 499 (2009) 28-31. https://doi.org/10.1016/j.msea.2007.09.102

[5] H.S. Liu, Z.W. Xing, J. Bao, B.Y. Song, Investigation of the Hot-Stamping Process for Advanced High-Strength Steel Sheet by Numerical Simulation, J. Mater. Eng. Perform. 19 (2009) 325-334. https://doi.org/10.1007/s11665-009-9510-y

[6] M. Merklein, J. Lechler, Investigation of the thermo-mechanical properties of hot stamping steels, J. Mater. Process. Tech. 177 (2006) 452-455. https://doi.org/10.1016/j.jmatprotec.2006.03.233

[7] B.L. Ma, M. Wan, X.D. Wu, Z.Y. Cai, K.S. Diao, J.Q. Han, Investigation on forming limit of advanced high strength steels (AHSS) under hot stamping conditions, J. Manuf. Process. 30 (2017) 320-327. https://doi.org/10.1016/j.jmapro.2017.10.001

[8] M.S. Mohamed, A.D. Foster, J. Lin, D.S. Balint, T.A. Dean, Investigation of deformation and failure features in hot stamping of AA6082: experimentation and modelling, Int. J. Mach. Tool. Manuf. 53 (2012) 27-38. https://doi.org/10.1016/j.ijmachtools.2011.07.005

[9] S. Bruschi, T. Altan, D. Banabic, P. Bariani, A. Brosius, J. Cao, A. Ghiotti, M. Khraisheh, M. Merklein, A. Tekkaya, Testing and modelling of material behaviour and formability in sheet metal forming, CIRP Annals-Manuf. Tech. 63 (2014) 727-749

[10] S.P. Keeler, Determination of forming limits in automotive stampings, Sheet Met. Ind. 42 (1965) 683-691. https://doi.org/10.4271/650535

[11] G.M. Goodwin, Application of strain analysis to sheet metal forming problems in the press shop, SAE Tech. Pap., 1968, pp. 380-387. https://doi.org/10.4271/680093

[12] S.K. Paul, Controlling factors of forming limit curve: A review, Adv. Industr. Manuf. Eng. 2 (2021). https://doi.org/10.1016/j.aime.2021.100033

[13] A. Atkins, Fracture in forming, J. Mater. Process. Tech. 56 (1996) 609-618. https://doi.org/10.1016/0924-0136(95)01875-1

[14] M. Dilmec, H.S. Halkaci, F. Ozturk, M. Turkoz, Detailed Investigation of Forming Limit Determination Standards for Aluminum Alloys, J. Testing Evaluat. 41 (2013). https://doi.org/10.1520/jte104356

[15] Z. Chen, G. Fang, J.-Q. Zhao, Formability evaluation of aluminum alloy 6061-T6 sheet at room and elevated temperatures, J. Mater. Eng. Perform. 26 (2017) 4626-4637. https://doi.org/10.1007/s11665-017-2895-0

[16] E. Affronti, C. Jaremenko, M. Merklein, A. Maier, Analysis of Forming Limits in Sheet Metal Forming with Pattern Recognition Methods. Part 1: Characterization of Onset of Necking and Expert Evaluation, Materials 11 (2018). https://doi.org/10.3390/ma11091495

[17] P. Bariani, S. Bruschi, A. Ghiotti, A. Turetta, Testing formability in the hot stamping of HSS, CIRP Annals - Manuf. Tech. 57 (2008) 265-268. https://doi.org/10.1016/j.cirp.2008.03.049

[18] L. Ying, T. Gao, H. Rong, X. Han, P. Hu, W. Hou, On the thermal forming limit diagram (TFLD) with GTN mesoscopic damage model for AA7075 aluminum alloy: Numerical and experimental investigation, J. Alloy. Compd. 802 (2019) 675-693. https://doi.org/10.1016/j.jallcom.2019.05.342

[19] H. Rong, P. Hu, L. Ying, W. Hou, J. Zhang, Thermal forming limit diagram (TFLD) of AA7075 aluminum alloy based on a modified continuum damage model: Experimental and theoretical investigations, Int. J. Mech. Sci. 156 (2019) 59-73. https://doi.org/10.1016/j.ijmecsci.2019.03.027

[20] BS EN ISO 12004, Metallic materials — Sheet and strip — Determination of forming-limit curves Part 2: Determination of forminglimit curves in the laboratory, BSI British Standards, 2008. https://doi.org/10.3403/bseniso12004

[21] R. Zhang, Z. Shi, V.A. Yardley, J. Lin, Experimental studies of necking and fracture limits of boron steel sheet under hot stamping conditions, J. Mater. Process. Tech. 302 (2022). https://doi.org/10.1016/j.jmatprotec.2021.117481

[22] R. Zhang, Z. Shi, Z. Shao, T.A. Dean, J. Lin, A novel spatio-temporal method for determining necking and fracture strains of sheet metals, Int. J. Mech. Sci. 189 (2021). https://doi.org/10.1016/j.ijmecsci.2020.105977

[23] R. Zhang, Z. Shi, Z. Shao, V.A. Yardley, J. Lin, An effective method for determining necking and fracture strains of sheet metals, MethodsX 8 (2021). https://doi.org/10.1016/j.mex.2021.101234

[24] R. Zhang, J. Jiang, J. Lin, V.A. Yardley, Investigation of variability in apparent values of materials properties in thermo-mechanical uniaxial tensile tests on sheet metals, J. Manuf. Process. 101 (2023) 737-754. https://doi.org/10.1016/j.jmapro.2023.06.005

[25] R. Zhang, Z. Shao, Z. Shi, T.A. Dean, J. Lin, Effect of cruciform specimen design on strain paths and fracture location in equi-biaxial tension, J. Mater. Process. Tech. 289 (2021). https://doi.org/10.1016/j.jmatprotec.2020.116932